

Highly Fluorescent Platinum(II) Organometallic Complexes of Perylene and Perylene Monoimide, with Pt σ -Bonded Directly to the Perylene Core

Sergio Lentijo, Jesús A. Miguel,* and Pablo Espinet*

IU CINQUIMA/Química Inorgánica, Facultad de Ciencias, Universidad de Valladolid, 47071 Valladolid, Spain

Received February 18, 2010

3-Bromoperylene (BrPer) or *N*-(2,5-di-*tert*-butylphenyl)-9-bromo-perylene-3,4-dicarboximide (BrPMI) react with [Pt(PEt₃)₄] to yield *trans*-[PtR(PEt₃)₂Br] (R = Per, **1a**; R = PMI, **1b**). Neutral and cationic perylenyl complexes containing a Pt(PEt₃)X group have been prepared from **1a,b** by substitution of the Br ligand by a variety of other ligands (NCS, CN, NO₃, CN^{*t*}Bu, PyMe). The X-ray structures of *trans*-[PtR(PEt₃)₂X] (R = Per, X = NCS (**2a**); R = PMI, X = NO₃ (**4b**); R = Per, X = CN^{*t*}Bu (**5a**)) show that the perylenyl fragment remains nearly planar and is arranged almost orthogonal to the coordination plane: The three molecules appear as individual entities in the solid state, with no π – π stacking of perylenyl rings. Each platinum complex exhibits fluorescence associated to the perylene or PMI fragments with emission quantum yields, in solution at room temperature, in the range 0.30–0.80 and emission lifetimes \sim 4 ns, but with significantly different emission maxima, by influence of the X ligands on Pt. The similarity of the overall luminescence spectra of these metalated complexes with the perylene or PMI strongly suggests a perylene-dominated intraligand π – π^* emissive state, metal-perturbed by interaction of the platinum fragment mostly via polarization of the Ar–Pt bond.

Introduction

Perylene dyes are well-known since 1913 as highly photo-stable pigments and dyes.¹ In recent years there has been a renewed interest in the design of new materials derived from the perylene chromophore because of their exceptional chemical and photochemical stability,² their high fluorescence quantum yields (sometimes close to 100%),³ and the large range of colors accessible by variation of the substitution pattern on the perylene core through high yield synthetic routes.⁴ These materials have been used in photovoltaic cells,⁵ xerography,⁶ optical switches,⁷ organic electronic devices such as organic light emitting diodes (OLED),⁸ laser dyes,⁹ or fluorescent collectors,¹⁰ as tracers in fluorescence analytical assays,¹¹ for charge transport in Langmuir–Blodgett films,¹² for

liquid crystals with special spectral properties,¹³ as fluorescent labeling reagents, or as fluorescent chemosensors,¹⁴ and recently, providing highly fluorescent J-aggregates.¹⁵

By far the majority of studies in this field elaborate around the readily accessible perylene tetracarboximides, with notable

*To whom correspondence should be addressed. E-mail: espinet@qi.uva.es (P.E.).

(1) (a) Zollinger, H. *Color Chemistry*, 3rd ed.; VCH: Weinheim, 2003; (b) Langhals, H. *Heterocycles* **1995**, *40*, 477. (c) Herbst, W.; Hunger, K. *Industrial Organic Pigments, Production Properties, Applications*; Wiley-VCH: Weinheim, 1997.

(2) Feiler, L.; Langhals, H.; Polborn, K. *Liebigs Ann.* **1995**, 1229. (3) (a) Würthner, F. *Chem. Commun.* **2004**, 1564. (b) Wasielewski, M. R. *J. Org. Chem.* **2006**, *71*, 5051.

(4) (a) Müllen, K.; Quante, H.; Benfaremo, N. *Polymeric Materials Encyclopedia*; Salamone, J. C., Ed.; CRC Press: Boca Raton, FL, 1996; p 4999. (b) Quante, H.; Geerts, Y.; Müllen, K. *Chem. Mater.* **1997**, *9*, 495.

(5) (a) Schmidt-Mende, L.; Fechtenkötter, A.; Mullen, K.; Moons, E.; Friend, R. H.; Mackenzie, J. D. *Science* **2001**, *293*, 1119. (b) Zhan, X.; Tan, Z.; Domercq, B.; An, Z.; Zhang, X.; Barlow, S.; Li, Y.; Zhu, D.; Kippelen, B.; Marder, S. R. *J. Am. Chem. Soc.* **2007**, *129*, 7246. (c) Breeze, A. J.; Salomon, A.; Ginley, D. S.; Gregg, B. A.; Tilmann, H.; Hörhold, H. *Appl. Phys. Lett.* **2002**, *81*, 3085.

(6) Loutfy, H. O.; Hor, A. M.; Kazmaier, P.; Tam, M. *J. Imaging Sci.* **1989**, *33*, 151.

(7) (a) O'Neil, M. P.; Niemczyk, M. P.; Svec, W. A.; Gosztola, D.; Gaines, G. L.; Wasielewski, M. R. *Science* **1992**, *257*, 63. (b) Yoo, B.; Jung, T.; Basu, D.; Dodabalapur, A.; Jones, B. A.; Facchetti, A.; Wasielewski, M. R.; Marks, T. J. *Appl. Phys. Lett.* **2006**, *88*, 082104/1. (c) Jones, B. A.; Ahrens, M. J.; Yoon, M. H.; Facchetti, A.; Marks, T. J.; Wasielewski, M. R. *Angew. Chem., Int. Ed.* **2004**, *43*, 6363.

(8) (a) Sauter, A.; Kaletas, B. K.; Schmid, D. G.; Dobrawa, R.; Zimine, M.; Jung, G.; Van Stokkum, I. H. M.; De Cola, L.; Williams, R. M.; Würthner, F. *J. Am. Chem. Soc.* **2005**, *127*, 6719. (b) Sugiyasu, K.; Fukita, N.; Shinkai, S. *Angew. Chem., Int. Ed.* **2004**, *43*, 1229.

(9) (a) Gvishi, R.; Reifeld, R.; Z. Bursheim, R. *Chem. Phys. Lett.* **1993**, *213*, 338. (b) Harriman, A.; Izzet, G.; Ziessel, R. *J. Am. Chem. Soc.* **2006**, *128*, 10868. (c) Yang, Y.; Lin, H.; Xu, H.; Wang, M.; Qian, G. *Opt. Commun.* **2008**, *281*, 5218.

(10) (a) Seybold, G.; Wangenblast, G. *Dyes Pigm.* **1989**, *11*, 303. (b) Alamiry, M. A. H.; Harriman, A.; Mallon, L. J.; Ulrich, G.; Ziesse, R. *Eur. J. Org. Chem.* **2008**, 2774.

(11) Langhals, H. *Heterocycles* **1995**, *40*, 477. (12) Burghard, M.; Fischer, C.; Schmelzer, M.; Roth, S.; Hanack, M.; Göpel, W. *Chem. Mater.* **1995**, *7*, 2104.

(13) Rohr, U.; Kohl, C.; Mullen, K.; van de Craats, A.; Warman, J. *J. Mater. Chem.* **2001**, *11*, 1789.

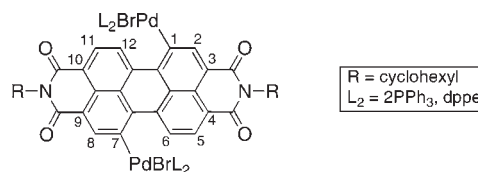
(14) (a) Nakaya, K.; Funabiki, K.; Shibata, K.; Matsui, M. *Bull. Chem. Soc. Jpn.* **2001**, *74*, 549. (b) Xie, J.; Ménand, M.; Maisonneuve, S.; Metivier, R. *J. Org. Chem.* **2007**, *72*, 5980.

(15) Kaiser, T. E.; Stepanenko, V.; Würthner, F. *J. Am. Chem. Soc.* **2009**, *131*, 6719.

contributions of Langhals', Müllen's, and Würthner's research groups.¹⁶ The optical and photophysical properties of the material are modified depending on the nature of the organic substituents in the aromatic core. As a result of these research efforts, many organic derivatives containing perylene have been reported, including commercial products used as dyes for polymers that cover all the rainbow's colors.

There are a few reports where the metal center is coordinated to a ligand that contains the perylene core,¹⁷ or π -bonded to the perylene core.¹⁸ Perylene-containing transition metal compounds with a direct σ -bond of the metal to the aromatic perylene core have been little studied, probably because attaching directly metal centers to aromatic cores of

Chart 1



organic chromophores is usually very detrimental for fluorescence (heavy-atom effect).^{19,20} Typically, the fluorescence quantum yield of complexes with ligands attached to late transition metals falls to values in the range 0–6% of those of the free ligands. This fairly general rule holds also for perylene-containing transition metal compounds of Pt or Pd.^{17a,b,21} Only recently two complexes have been reported, with Pd bonded to the bay region (1, 6, 7, and 12 position of perylene diimide unit) of a perylene diimide,²² showing much higher quantum yields ($\Phi = 0.65$ and 0.22).

A problem in the study of perylene derivatives is the poor solubility of the compounds. A strategy to alleviate the problem is to attach solubilizing side chains to the perylene, but this approach is synthetically very demanding and usually leads to mixtures of isomers.²³ Our strategy to enhance the solubility was to incorporate, at a side position of the perylene core, a metal center with appropriate ligands. The presence of the metal and their ancillary ligands should, additionally, offer an easy way to modify the optoelectronic properties of the material, and could offer an efficient tool to create new structural and functional motifs, significantly widening the diversity of photofunctional systems available. In the course of this project and following the same idea, two complexes were reported by the Rybtchinski group, with Pd directly attached to the 1,7 aromatic positions of a perylene diimide (Chart 1).²²

Here we report the synthesis of Pt(II) complexes with the platinum σ -bonded to position 3 of the perylene core, obtained by oxidative addition of either 3-bromoperylene (BrPer) or *N*-(2,5-di-*tert*-butylphenyl)-9-bromo-perylene-3,4-dicarboximide (BrPMI) to [Pt(PET₃)₄], and by substitution of the Br ligand in the products by a variety of other ligands (NCS, CN, NO₃, CN^tBu, PyMe), affording neutral and cationic complexes. Our initial source of perylene core was BrPMI, meant to provide better solubility to the metal derivatives, but soon it was realized that the presence of PET₃ was enough to induce good solubility in the derivatives of unmodified BrPer (sometimes the solubility is even higher for Per than for PMI derivatives). This unexpected result offered an interesting simplification for further studies, so some of the complexes were made only with Per. The effects of combining the perylene core with the electron density of metal center and the ancillary ligands coordinated trans to the perylene are discussed.

(19) Yersin, H.; Strasser, J. *Coord. Chem. Rev.* **2000**, *208*, 331.

(20) Chandra, A. K.; Turro, N. J.; Lyons, A. L., Jr.; Stone, P. J. *Am. Chem. Soc.* **1978**, *100*, 4964.

(21) (a) Hu, J.; Lin, R.; Yip, J. H. K.; Wong, K. Y.; Ma, D. L.; Vittal, J. J. *Organometallics* **2007**, *26*, 6533. (b) Heng, W. Y.; Hu, J.; Yip, J. H. K. *Organometallics* **2007**, *26*, 6760. (c) Hu, J.; Yip, J. H. K.; Ma, D. L.; Wong, K. Y.; Chung, W. H. *Organometallics* **2009**, *28*, 51. (d) Tennyson, E. G.; Smith, R. C. *Inorg. Chem.* **2009**, *48*, 11483. (e) Wilson, J. J.; Lopes, J. F.; Lippard, S. J. *Inorg. Chem.* **2010**, *49*, 5303. (f) Christoforou, A. M.; Marzilli, P. A.; Marzilli, L. G. *Inorg. Chem.* **2006**, *45*, 6771. (g) Bai, D. R.; Romero-Nieto, C.; Baumgartner, T. *Dalton Trans.* **2010**, *39*, 1250.

(22) Weissman, H.; Shirman, E.; Ben-Moshe, T.; Cohen, R.; Leitun, G.; Shimon, L. J. W.; Rybtchinski, B. *Inorg. Chem.* **2007**, *46*, 4790.

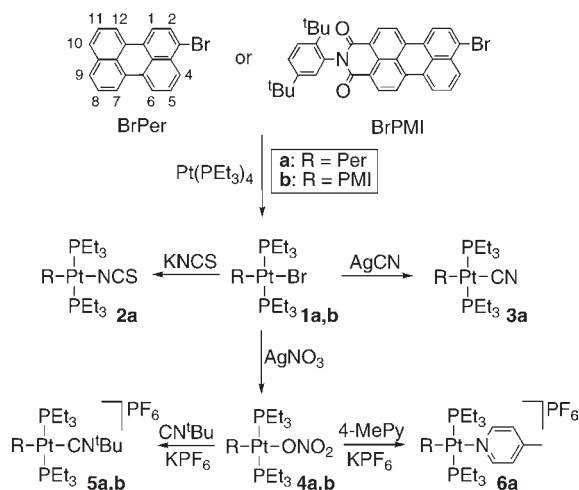
(23) Schlichting, P.; Rohr, U.; Müllen, K. *Liebigs Ann./Rec.* **1997**, 395.

(16) A selection of recent articles: (a) Langhals, H.; Jäschke, H.; Bastani-Oskoui, H.; Speckbacher, M. *Eur. J. Org. Chem.* **2005**, 4313. (b) Langhals, H. *Helv. Chim. Acta* **2005**, *88*, 1309. (c) Debije, M. G.; Chen, Z. J.; Neder, R. B.; Watson, M. M.; Mullen, K.; Würthner, F. *J. Mater. Chem.* **2005**, *15*(12), 1270. (d) Nolde, F.; Qu, J.; Kohl, C.; Pschirer, N. G.; Reuther, E.; Mullen, K. *Chem.—Eur. J.* **2005**, *11*, 3959. (e) Nolde, F.; Pisula, W.; Müller, S.; Kohl, C.; Mullen, K. *Chem. Mater.* **2006**, *18*, 16. (f) Langhals, H.; El-Shishtawy, R.; von Unold, P.; Rauscher, M. *Chem.—Eur. J.* **2006**, *12*, 4642. (g) Langhals, H.; Krotz, O. *Angew. Chem., Int. Ed.* **2006**, *45*, 4444. (h) Avlasevich, Y.; Müller, S.; Erk, P.; Mullen, K. *Chem.—Eur. J.* **2007**, *13*, 6555. (i) Oesterling, I.; Mullen, K. *J. Am. Chem. Soc.* **2007**, *129*, 4595–4605. (j) Avlasevich, Y.; Mullen, K. *J. Org. Chem.* **2007**, *72*, 26. (k) Fron, E.; Bell, T. D. M.; Van Vooren, A.; Schweitzer, G.; Cornil, J.; Beljonne, D.; Toele, P.; Jacob, J.; Mullen, K.; Hofkens, J.; Van der Auweraer, M.; De Schryver, F. *J. Am. Chem. Soc.* **2007**, *129*(3), 610. (l) Kaiser, T. E.; Stepanenko, V.; Würthner, F. *Angew. Chem., Int. Ed.* **2007**, *46*, 5541. (m) Chen, Z.; Baumesteir, U.; Tschierske, C.; Würthner, F. *Chem.—Eur. J.* **2007**, *13*, 450. (n) Flamigni, L.; Ventura, B.; Tasior, M.; Becherer, T.; Langhals, H.; Gryko, D. T. *Chem.—Eur. J.* **2008**, *14*, 169. (o) Langhals, H.; Rauscher, M.; Strbe, J.; Kuck, D. *J. Org. Chem.* **2008**, *73*, 1113. (p) Peneva, K.; Mihov, G.; Nolde, F.; Rocha, S.; Hotta, J.; Braeckmans, K.; Hofkens, J.; Uji-i, H.; Herrmann, A.; Mullen, K. *Angew. Chem., Int. Ed.* **2008**, *47*, 3372. (q) Peneva, K.; Mihov, G.; Herrmann, A.; Zarrabi, N.; Börsch, M.; Duncan, T. M.; Mullen, K. *J. Am. Chem. Soc.* **2008**, *130*, 5398. (r) Hansen, M. R.; Schnitzler, T.; Pisula, W.; Graf, R.; Mullen, K.; Spiess, H. W. *Angew. Chem., Int. Ed.* **2009**, *48*, 4621. (s) Rabirian, R.; Palermo, V.; Liscio, A.; Schwartz, E.; Otten, M. B. J.; Finlayson, C. E.; Treossi, E.; Friend, R. H.; Calestani, G.; Mullen, K.; Nolte, R.; Rowan, A.; Samori, A. *J. Am. Chem. Soc.* **2009**, *131*, 7055. (t) Li, C.; Shoneboom, J.; Liu, Z.; Pschirer, N. G.; Erk, P.; Herrmann, A.; Mullen, K. *Chem.—Eur. J.* **2009**, *15*, 878. (u) Langhals, H.; Esterbauer, A. *J. Chem.—Eur. J.* **2009**, *15*, 4793. (v) Oh, J.; Sun, Y.; Schmidt, R.; Toney, M. F.; Nordlund, D.; Könemann; Würthner, F.; Bao, Z. *Chem. Mater.* **2009**, *21*, 5508. (w) Zhao, H.; Pfisher, J.; Settles, V.; Renz, M.; Kaupp, M.; Dehm, V.; Würthner, F.; Fink, R. F.; Engels, B. *J. Am. Chem. Soc.* **2009**, *131*, 15660. (x) Schmidt, R.; Oh, J.; Sun, J.; Deppish, M.; Krause, A. M.; Radacki, K.; Braunschweig, H.; Konemann, M.; Erk, P.; Bao, Z.; Würthner, F. *J. Am. Chem. Soc.* **2009**, *131*, 6215.

(17) (a) Rachford, A. A.; Goeb, S.; Castellano, F. *J. Am. Chem. Soc.* **2008**, *130*, 2766. (b) Rachford, A. A.; Goeb, S.; Ziessel, R.; Castellano, F. *Inorg. Chem.* **2008**, *47*, 4348. (c) Zhu, W.; Fan, L. *Dyes Pigm.* **2008**, *76*, 663. (d) Qvortrup, K.; Bond, A. D.; Nielsen, A.; McKenzie, C. J.; Kilsa, K.; Nielsen, M. B. *Chem. Commun.* **2008**, 1986. (e) Vilaca, G.; Barathieu, K.; Jousseau, B.; Toupance, T.; Allouchi, H. *Organometallics* **2003**, *22*, 4584. (f) Cuffe, L.; Hudson, R. D. A.; Gallagher, J. F.; Jennings, S.; McAdam, C. J.; Connelly, R. B. T.; Manning, A. R.; Robinson, B. H.; Simpson, J. *Organometallics* **2005**, *24*, 2051. (g) Suenaga, Y.; Kuroda-Sowa, T.; Munakata, M.; Maekawa, M. *Polyhedron* **1998**, *17*, 2207. (h) Qvortrup, K.; Bond, A. D.; Nielsen, A.; McKenzie, C. J.; Kilsa, K.; Nielsen, M. B. *Chem Commun.* **2008**, 1986. (i) Würthner, F.; Sautter, A.; Schmid, D.; Weber, P. J. A. *Chem.—Eur. J.* **2001**, *7*, 894. (j) You, C. C.; Hippus, C.; Grüne, M.; Würthner, F. *Chem.—Eur. J.* **2006**, *12*, 7510. (k) Rodríguez-Morgade, M. S.; Torres, T.; Atienza-Castellanos, C.; Guldí, D. M. *J. Am. Chem. Soc.* **2006**, *128*, 15145. (l) Jiménez, A. J.; Spänig, F.; Rodríguez-Morgade, M. S.; Ohkubo, K.; Fukuzumi, S.; Guldí, D. M.; Torres, T. *Org. Lett.* **2007**, *9*, 2481. (m) Goretzki, G.; Davies, E. D.; Argent, S. P.; Warren, J. E.; Blake, A. J.; Champness, N. R. *Inorg. Chem.* **2009**, *48*, 10264. (n) Gebers, J.; Rolland, D.; Frauenrath, H. *Angew. Chem., Int. Ed.* **2009**, *48*, 4480.

(18) (a) Porter, L. C.; Polam, J. R.; Bodige, S. *Inorg. Chem.* **1995**, *34*, 998. (b) Shibusaki, T.; Komine, N.; Hirano, M.; Komiya, S. *J. Organomet. Chem.* **2007**, *692*, 2385. (c) Arrais, A.; Diana, E.; Gervasio, G.; Gobetto, R.; Marabellio, D.; Stanghellini, P. L. *Eur. J. Inorg. Chem.* **2004**, 1505. (d) Murahashi, T.; Uemura, T.; Kurosawa, H. *J. Am. Chem. Soc.* **2003**, *125*, 8436. Murahashi, T.; Kato, N.; Uemura, T.; Kurosawa, H. *Angew. Chem., Int. Ed.* **2007**, *46*, 3509.

Scheme 1



Results and Discussion

Synthesis and Characterization. Following a literature procedure, commercial perylene was brominated with *N*-bromosuccinimide (NBS) in dimethylformamide (DMF) to yield 3-bromoperylene (BrPer).²⁴ *N*-(2,5-di-*tert*-butylphenyl)-9-bromo-perylene-3,4-dicarboximide (BrPMI), was obtained by bromination of PMI with bromine in chlorobenzene.²⁵ The syntheses of the platinum complexes **1–6** are outlined in Scheme 1.

The complexes **1a,b** were easily prepared in good yield, as yellow solids, by oxidative addition of BrPer or BrPMI to [Pt(PEt₃)₄] in toluene. Metathesis of **1a** with one molar equivalent of KSCN, in acetone, led to SCN for Br exchange. The value 2099 cm⁻¹ for $\nu(\text{CN})$ suggests N-coordination of the thiocyanato group,²⁶ which was confirmed by X-ray diffraction methods (see later). Complexes **1a,b** reacted with silver salts AgCN or AgNO₃, in acetone, yielding **3a** or **4a,b** respectively in good yield. For the cyanide complex **3a**, $\nu(\text{C}\equiv\text{N})$ is observed at 2116 cm⁻¹. The facile displacement of the nitrate group in compounds **4a,b** by other ligands was used to obtain cationic complexes.²⁷ Thus, **5a,b** and **6a** were obtained in high yield when **4a,b** was treated with an equimolar amount of *tert*-butylisocyanide or 4-methylpyridine, respectively, and KPF₆ was added to help for crystallization of the cation complex with a larger anion. The IR spectra of **5a,b** show a $\nu(\text{C}\equiv\text{N})$ absorption (ca. 2195 cm⁻¹) at wavenumbers about 55 cm⁻¹ higher than for the free isocyanide as an effect of coordination to platinum(II).²⁸ The IR

spectra of the derivatives with PMI show additionally the expected $\nu(\text{C}=\text{O})$ absorptions at about 1699 and 1656 cm⁻¹.

The compounds were isolated as brown or yellow solids for the perylene complexes, and red or pink solids for the PMI compounds. They are soluble in organic solvents such as chloroform, dichloromethane, toluene, acetone, and tetrahydrofuran (THF), but insoluble in hexane, diethyl ether, methanol, and ethanol. The elemental analysis, yields, relevant IR data, ¹H and ³¹P{¹H}NMR data for the complexes are given in the Experimental Section.

The ¹H NMR spectra of the metal complexes are very similar for each family. The aromatic resonances are complex, because of the lack of symmetry of the compounds, and were assigned with the help of COSY and NOESY experiments. The ³¹P{¹H} NMR spectra of all the metal complexes are consistent with a *trans* arrangement of the phosphines and show a sharp singlet with ¹⁹⁵Pt satellites in the range 17.5–11.0 ppm. The ³¹P chemical shifts are very similar for Per and PMI (a bit smaller for the later), but quite sensitive to the fourth ligand: ONO₂ (17.24 ppm) < NCS (14.56) < CN^tBu (12.32) < Br (12.19) < Py-Me (11.74) < CN (11.16) for the perylene complexes; ONO₂ (17.02 ppm) < Br (12.12) < CN^tBu (11.75) for the PMI derivatives. The deshielding is particularly marked for the nitrate complexes **4a,b**. The ¹J_{PtP} values are in the range 2350–2850 Hz: ONO₂ (2841 Hz) > NCS (2740) > Br (2704) > Py-Me (2662) > CN (2590) > CN^tBu (2413) for the perylene complexes; ONO₂ (2795 Hz) > Br (2666) > CN^tBu (2382) for the PMI derivatives. This range is typical of a *trans*-P-Pt-P configuration about the platinum metal centers.²⁹

Crystal Structures. X-ray quality crystals could be obtained for the complexes **2a**, **4b**, and **5a**. Their structures were determined by single-crystal X-ray diffraction methods and are shown in Figure 1. Selected bond lengths and angles are given in Table 1. Data collection and refinement parameters are listed in the Experimental Section.

In general, there are no significant changes in bond lengths and angles of the perylene skeleton compared to the X-ray structure reported for perylene.³⁰ The Pt(II) center shows, in all complexes, a slightly distorted square planar geometry. Confirming the NMR studies, the crystal structures of **2a**, **4b**, and **5a** show that the triethylphosphine ligands are in *trans* configuration, with P(1)–Pt–P(2) angles in the range 174–178°. The Per or PMI fragment is nearly planar and is arranged almost orthogonal to the coordination plane (the dihedral angles are 89.72° (**2a**), 84.65° (**4b**), 84.62° (**5a**)). In **4b** the imide group and the N-aryl with the 2,5-di-*tert*-butyl groups are planar and orthogonal to each other (dihedral angle 87.48°). The plane of the NO₃ ligand is also roughly perpendicular to the coordination plane (89.16°). The Pt(1)–C(1) distances are in concordance with the *trans*-influence of L: CN^tBu (**5a**, 2.057(6) Å) > NCS (**2a**, 2.003(4) Å) > ONO₂ (**4b**, 1.995(14) Å). The Pt–P (2.2979(14)–2.3264(19) Å) bond lengths are within normal ranges.

(29) (a) Kim, D.; Paek, J. H.; Jun, M.-J.; Lee, J. Y.; Kang, S. O.; Ko, J. *Inorg. Chem.* **2005**, *44*, 7886. (b) Kryshchenko, Y. K.; Seidel, S. R.; Arif, A. M.; Stang, P. J. *J. Am. Chem. Soc.* **2003**, *125*, 5193.

(30) Nther, C.; Bock, H.; Havlas, Z.; Hauck, T. *Organometallics.* **1998**, *17*, 4707.

(24) (a) Mitchell, R. H.; Lai, Y. H.; Williams, R. V. *J. Org. Chem.* **1979**, *44*, 4733. (b) Lapuyade, R.; Pereyre, J.; Garrigues, P. C. *R. Acad. Sci. Ser. II* **1986**, *303*, 903.

(25) (a) Schlichting, P.; Rohr, U.; Müllen, K. *Liebigs Ann./Rec.* **1997**, 395. (b) Tomozaki, K.; Thamyongkit, P.; Loewe, R. S.; Lindsey, J. S. *Tetrahedron* **2003**, *59*, 1191.

(26) Tau, K. D.; Meek, D. W. *Inorg. Chem.* **1978**, *18*, 3574. (27) (a) Kuehl, C.; Huang, S.; Stang, P. *J. Am. Chem. Soc.* **2001**, *123*, 9634. (b) Addicott, C.; Das, N.; Stang, P. *Inorg. Chem.* **2004**, *43*, 5335.

(28) (a) Hartley, F. R. In *Comprehensive Organometallic Chemistry*; Abel, E. W., Stone, F. G. A., Wilkinson, G., Eds.; Pergamon Press: Oxford, U. K., 1982; Vol. 6, p 498. (b) Kaharu, T.; Tanaka, T.; Sawada, M.; Takahashi, S. *J. Mater. Chem.* **1994**, *4*, 859. (c) Coco, S.; Díez-Expósito, F.; Espinet, P.; Fernández-Mayordomo, C.; Martín-Álvarez, J. M.; Levelut, A. M. *Chem. Mater.* **1998**, *10*, 3666. (d) Díez, A.; Forniés, J.; Fuertes, S.; Lalinde, E.; Larraz, C.; López, J. A.; Martín, A.; Moreno, M. T.; Sicilia, V. *Organometallics.* **2009**, *28*, 1705.

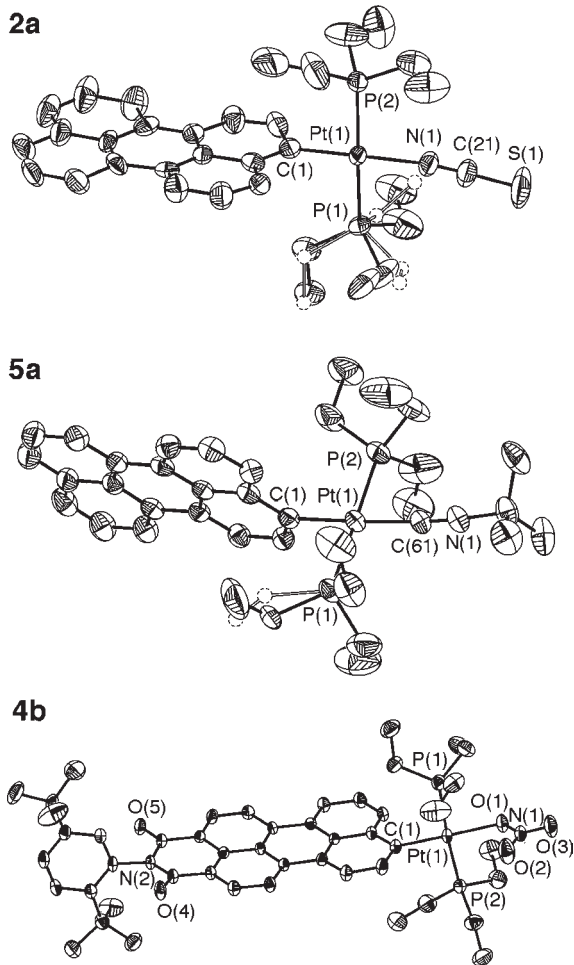


Figure 1. ORTEPs of the crystal structures of the molecule (**2a**, **4b**) or the cation (**5a**) of compounds **2a**, **4b**, and **5a**. The ellipsoids are shown at 30% probability (H atoms are omitted for clarity). The ellipsoids of the minor component of the disordered structure of **2a** and **5a** have been omitted for clarity. For **5a**, the anion PF_6^- and co-crystallized CH_2Cl_2 have been omitted.

Complex **2a** features N-bonded thiocyanate, with the Pt–N(1)–C(21) and N(1)–C(21)–S(1) bond angles only slightly deviated from linearity (173.1(13) and 177.5(19), respectively). Reflecting the high *trans*-influence of the perylenyl group, the Pt–N distance (2.052(12) Å) is longer than those found in most thiocyanato-platinum(II) complexes,³¹ but comparable to that found in the few related *trans* R–Pt–NCS complexes reported.³² The Pt–O distances in **4b** are not significantly different (ca. 2.15–2.17 Å) and are similar to those found in related complexes.^{27,29} In **5a**, the Pt–C(61) distance (1.983(6) Å) is within the range of those reported for other *tert*-butylisocyanide platinum complexes, with aryls in *trans* position.³³

The crystal networks of the complexes show that the potential aggregation of the molecules, often found in

Table 1. Selected Interatomic Distances (Å) and Angles (deg) for the Complexes **2a**, **4b**, and **5a**

	2a	4b	5a · CH_2Cl_2
Pt(1)–C(1)	1.995(14)	2.003(4)	2.057(6)
Pt(1)–P(1)	2.314(3)	2.3080(14)	2.3264(19)
Pt(1)–P(2)	2.319(3)	2.2979(14)	2.3189(19)
Pt(1)–N(1)	2.057(11)	2.151(3)	
N(1)–C(21)	1.130(16)		
C(21)–S(1)	1.630(16)		
Pt(1)–C(61)			1.983(6)
C(61)–N(1)			1.131(7)
N(1)–C(62)			1.471(8)
O(1)–N(1)		1.263(6)	
C(1)–Pt(1)–X	177.1(5)	178.36(16)	177.5(2)
C(1)–Pt(1)–P(1)	89.4(3)	91.86(14)	90.55(16)
X–Pt(1)–P(1)	88.6(3)	86.69(11)	91.93(18)
C(1)–Pt(1)–P(2)	90.4(3)	92.66(14)	87.53(16)
X–Pt(1)–P(2)	91.4(3)	88.84(11)	89.98(18)
P(1)–Pt(1)–P(2)	174.71(13)	174.33(5)	177.62(6)
N(1)–C(21)–S(1)	177.5(19)		
C(21)–N(1)–Pt(1)	173.1(13)		
C(61)–N(1)–C(62)			175.9(7)
N(1)–C(61)–Pt(1)			175.6(6)
perylene plane/coord. plane angle	89.72	84.65	84.62

organic compounds with extended aromatic cores, is hindered here by the bulky PET_3 ligands, and the N-aryl with two 2,5-di-*tert*-butyl groups in **4b**. In effect, all the molecules appear as basically individual objects with no π – π stacking of perylenyl rings. Notwithstanding that, some intermolecular contacts (O3–C21 (3.005 Å) and O4–H51A (2.457 Å) distances are smaller than the sum of the van der Waals radii) have been detected in **4b**.

Photophysical Studies

(a). **UV–vis Absorption Spectra.** The UV–vis absorption and fluorescence behavior of the complexes has been investigated in solution and in the solid state to study the influence of the $\text{PtX}(\text{PET}_3)_2$ group on the photophysical properties of the Per or PMI. The platinum complexes are fairly stable in solution but very slowly decompose with change of the color of the solution after several days. The decomposition is very slow, and the UV–vis spectrum of **1a** in chloroform remains constant after 24 h.

The absorption spectra of perylene, BrPer, PMI, BrPMI, and their corresponding platinum(II) complexes are shown in Figure 2. The quantitative data are summarized in Table 2.

The UV–vis absorptions of perylene, BrPer, and their related complexes **1a–6a** display very similar profiles, exhibiting absorptions dominated by the π – π^* transition of the perylene moiety. The spectra consist of a strong absorption at about 250 nm, with a more or less defined shoulder, and three other broad overlapped absorptions in the range 370–500 nm. These lowest energy bands of BrPer and **1a–6a** have similar band shapes that resemble the spectrum of perylene (with very intense vibronic bands at 360–460 nm) with a moderate red-shifted of 360–1400 cm^{-1} relative to perylene. Moreover, the lowest energy bands of **1a** are fairly insensitive to solvent polarity, as they are red-shifted less than 200 cm^{-1} when the solvent is changed from toluene to DMF (see the Supporting Information, Figure S1).

The shift to higher wavelength (red shift for short) observed in the complexes, relative to perylene indicates that the perturbation exerted on the perylene by the $\text{Pt}(\text{PET}_3)_2\text{X}$ groups is stronger (in the range 850–1410 cm^{-1}) than that of Br (360 cm^{-1}), as observed also in related perylenyl

(31) (a) Kishi, S.; Kato, M. *Inorg. Chem.* **2003**, *42*, 8728. (b) Johanson, M. H.; Otto, S.; Oskarsson, A. *Acta Crystallogr., Sect. B. Sci.* **2002**, *58*, 244.

(32) (a) Otto, S.; Roodt, A. *Acta Crystallogr., Sect. E. Struct. Rep. Online* **2005**, *61*, 1545. (b) Behrens, U.; Hoffmann, K.; Kopf, J.; Moritz, J. *J. Organomet. Chem.* **1976**, *117*, 91.

(33) See for example: (a) Ackermann, M. N.; Ajmera, R. K.; Barnes, H. E.; Gallucci, J. C.; Wojcicki, A. *Organometallics*. **1999**, *18*, 787. (b) Huh, H. S.; Lee, Y. K.; Lee, S. W. *J. Mol. Struct.* **2006**, *789*, 209. (c) Kim, Y. J.; Choi, E. H.; Lee, S. W. *Organometallics*. **2003**, *22*, 3316.

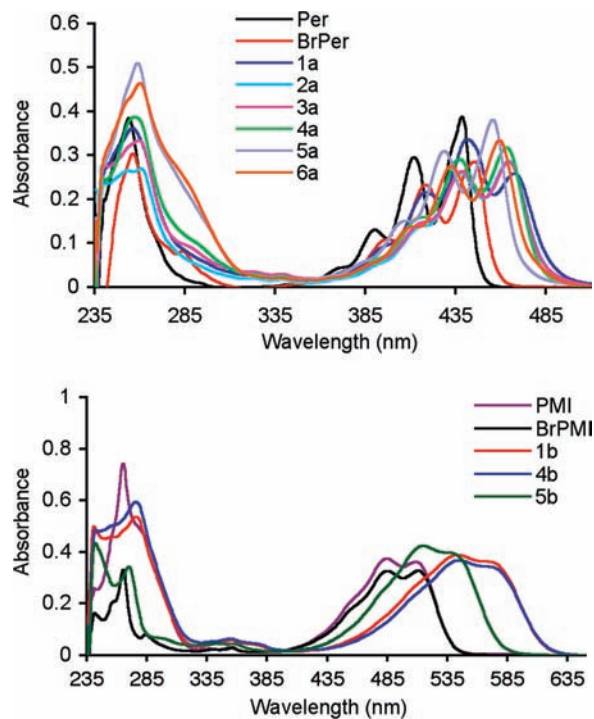


Figure 2. (top) Absorption spectra of perylene, BrPer and their platinum complexes **1a–6a**, recorded in CHCl_3 solution ($\sim 10^{-5}$ M) at room temperature. (bottom) Absorption spectra of PMI, BrPMI, and their platinum complexes **1b**, **4b**, and **5b** in CHCl_3 at room temperature.

Table 2. UV–vis Absorption of Perylene, BrPer, BrPMI, and Their Platinum Complexes, in Chloroform at 298 K

compound	λ/nm ($10^{-3} \epsilon/\text{M}^{-1} \text{cm}^{-1}$)
perylene	439 (35.2) 412 (26.8), 391 (11.9), 254 (34.9)
BrPer	446 (28.6), 419 (23.3), 397 (10.9), 257 (30.4)
1a	468 (25.8), 441 (33.6), 419 (21.5), 256 (36.1)
2a	464 (28.4), 439 (26.3), 259 (33.3), 240 (28.6)
3a	463 (31.7), 437 (29.1), 237 (38.7), 240 (24.9)
4a	464 (28.8), 438 (26.0), 260 (27.0), 253 (26.5)
5a	456 (38.0), 429 (30.9), 259 (51.0)
6a	459 (33.4), 432 (27.5), 260 (46.4)
PMI	512(33.6), 489 (35.3) 264 (32.8)
BrPMI	511 (32.6), 485 (32.5), 265 (33.0), 241 (16.2)
1b	570 (36.2), 543 (38.8), 276 (53.6), 240 (50.0)
4b	570 (34.3), 544 (36.7), 276 (59.3)
5b	539 (39.6), 515 (42.4), 270 (34.2), 242 (43.4)

complexes.^{21b} The shift produced by cationic $[\text{Pt}(\text{PEt}_3)_2\text{X}]^+$ groups is lower than observed for neutral complex fragments: **5a**⁺ (850 cm^{-1}) < **6a**⁺ (990 cm^{-1}) < **4a** ~ **2a** ~ **3a** (1180 cm^{-1}) < **1a** (1410 cm^{-1}). This is the expected result, as a cationic charge in the platinum fragment should contract the d orbitals of the platinum and reduce the magnitude of the interaction with the perylene orbitals. Similar electronic effects have been found in platinum-anthracenyl complexes (see further discussion of these concepts in the last paragraph of this paper preceding the conclusions).^{21a}

The PMI neutral derivatives **1b** and **4b** are deep purple, with an intense purple fluorescence in solution. The cationic complex **5b** is red with a strong orange fluorescence in solution. The electronic spectra **1b**, **4b**, and **5b** show a profile which differs from that of the perylene complexes (as PMI differs also from Per) in the higher sharpness of the vibronic structure for the PMI derivatives; it is frequent that the vibrational structure is obscured when the aromatic residue

Table 3. Emission and Excitation in Chloroform Solution (10^{-5} M) and in the Solid State (KBr pellet) at 298 K

compound	CHCl_3		CH_2Cl_2		KBr	
	$\lambda_{\text{ex}}/\text{nm}$	$\lambda_{\text{em}}/\text{nm}$	Φ^a	τ/ns	$\lambda_{\text{ex}}/\text{nm}$	$\lambda_{\text{em}}/\text{nm}$
BrPer	435	445, 468, 504sh				
1a	442	485, 516, 558sh	0.70	4.65	470	553
2a	464	482, 511, 555sh	0.78	4.48	480	553
3a	462	480, 510, 545sh	0.70	5.02	460	547
4a	468	488, 517, 556sh	0.77	4.26	480	547
5a	450	467, 496, 531sh	0.43	1.88	474	545
6a	455	472, 501, 539sh	0.67	4.19	450	534
BrPMI	512	542, 577, 634sh	0.98 ^b			
1b	561, 602	618, 660	0.30 ^c	4.46	457	685
4b	542	618, 660	0.34 ^c	4.62	457	669
5b	517, 540	581, 620	0.78 ^c	4.65	462	654

^a Determined relative to perylene in ethanol ($\Phi_{\text{P}} = 0.92$)³⁴ and using an excitation wavelength of 409 nm in CH_2Cl_2 . ^b Taken from the literature.³⁵ ^c Determined using Rhodamine B in ethanol ($\Phi_{\text{R}} = 0.70$)³⁶ and using an excitation wavelength of 510 nm in CH_2Cl_2 .

is engaged in more extensive conjugation. While the perturbation produced by the Br atom of the PMI lowest energy band is very small, the $\text{Pt}(\text{PEt}_3)_2\text{X}$ group produces a clear red-shift of the visible bands ranging from 980 cm^{-1} for the cationic complex **5b** ($\text{X} = \text{CN}^t\text{Bu}$) to 1990 cm^{-1} for the neutral compounds **1b** ($\text{X} = \text{Br}$) and **4b** ($\text{X} = \text{ONO}_2$) (See Figure 2), with bigger bathochromic shifts than perylenyl complexes. This red shift is somewhat larger than in the case of the perylene derivatives.

(b). Luminescence Spectra. The luminescence spectroscopic properties of the ligands and the platinum complexes at room temperature in chloroform or in the solid state (KBr dispersion or pellets) are listed in Table 3. Both neutral and cationic complexes exhibit strong fluorescence in solution and have well-defined vibronic fine structure (See Figure 3).

The platinum metal complexes display luminescent properties, showing that the metal does not impose a heavy atom effect. The similarity of the overall luminescence spectra of these metalated complexes with the perylene strongly suggests an intraligand $\pi-\pi^*$ transition where the ligand orbitals have been slightly modified by the presence of the metal. On the basis of the similar Stokes shifts³⁷ between absorption and emission for the ligands and the complexes (lower than 1000 cm^{-1}), the luminescence observed can be assigned to $\pi-\pi^*$ fluorescence, which was supported by the fact that the emission properties remain unchanged in the presence of air, and confirmed with the measurement of their emission lifetimes $\sim 4 \text{ ns}$, (see Table 2).

For the perylene derivatives, Figure 3 shows normalized emission spectra in chloroform solution of the complexes **1a–6a**. The cationic complexes **5a** and **6a** ($\lambda_{\text{max}} \sim 470 \text{ nm}$) are less red-shifted relative to perylene than the neutral compound **1a–4a** ($\lambda_{\text{max}} \sim 485 \text{ nm}$), as expected

(34) Montalti, M.; Credi, A.; Prodi, L.; Gandolfini, M. T. *Handbook of Photochemistry*, 3rd ed.; CRC Press LLC: Boca Raton, FL, 2005.

(35) Baffre, J.; Ordronneau, L.; Leroy-Lhez, S.; Hudhomme, P. *J. Org. Chem.* **2008**, *73*, 6142.

(36) López-Arbeloa, F.; Ruiz-Ojeda, P.; López-Arbeloa, I. *J. Lumin.* **1989**, *44*, 105.

(37) (a) Lakowicz, J. R. *Principles of Fluorescence Spectroscopy*; Plenum Press: New York, 1983. (b) Guilbault, G. G. *Fluorescence*, 2nd ed.; Marcel Dekker, Inc.: New York, 1990.

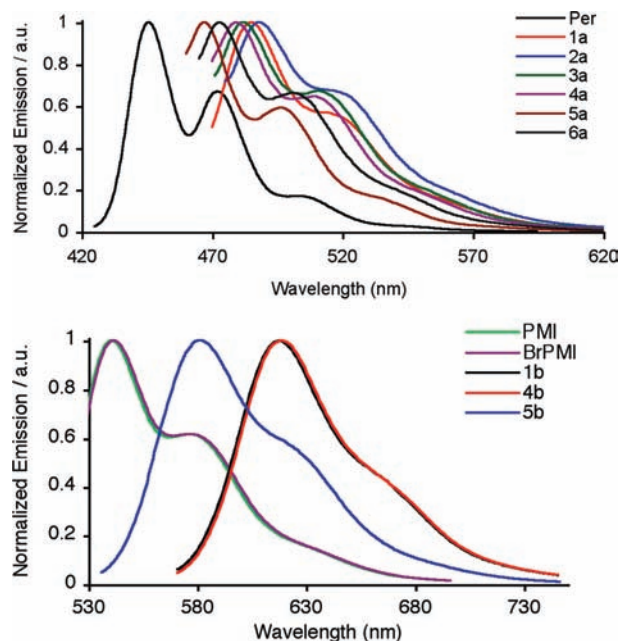


Figure 3. Emission spectra recorded in CHCl_3 solution ($\sim 10^{-5}$ M) at room temperature (top) Per and complexes **1a–6a**. (bottom) PMI, BrPMI, and complexes **1b**, **4b** and **5b**.

from the fact that the fluorescence spectrum should be a mirror image of the absorption spectrum. At low temperature (77 K) in solution (whether in chloroform, 2-Me-THF or toluene) the spectrum for **1a** is almost identical to that of the room temperature solution, but with the shoulders resolved as a sharp peak (Supporting Information, Figure S4). In the solid-state the intensity of emission bands decreases noticeably, and the emission spectrum displays, as expected, a broad maximum that is shifted to lower energy ($> 2700 \text{ cm}^{-1}$ for **1a**) with respect to the solution emissions.³⁸ The nearly identical emission spectra of **1a** in different solvents, at room temperature (in Supporting Information, Figure S5), indicates that the fluorescence of the perylenyl derivatives is hardly sensitive to the polarity of the solvent, consistent with the assignment of the emission.

For the PMI derivatives, both PMI and BrPMI exhibit very similar emission spectra with $\lambda_{\text{max}} = 542 \text{ nm}$ with a vibronic structure similar to perylene but not as well-defined (Figure 3 (bottom)). The complexes **1b**, **4b**, and **5b** also show strong luminescence and exhibit the characteristic fluorescence of the PMI, but with significant low energy shifts, bigger Stokes shifts, and less resolution of the vibronic structure. Differently from the perylene complexes (Figure 3 (top)), and similar to perylene diimides³⁹ and BrPMI, the bands of **1b** are somewhat sensitive to solvent variation from toluene to acetonitrile ($< 600 \text{ cm}^{-1}$ for PMI and $< 800 \text{ cm}^{-1}$ for the complexes (Supporting Information, Figure S4)). The emission maxima in complexes **1b** and **4b** appear at 618 nm, 76 nm (2270 cm^{-1}) red-shifted from PMI. In the cationic complex **5b**, this red shift is again lower than in the neutral derivatives, and its emission maximum appears at 581 nm, shifted 39 nm, 1240 cm^{-1} (See Figure 3). At low temperature (77 K) the

Table 4. Half-Wave Redox Potentials for Per and PMI Derivatives^a

compd	$E_{1\text{ox}}$	$E_{1\text{r}}$	$E_{2\text{r}}$
1a	0.73		
2a	0.78		
3a	0.76		
4a	0.78		
5a	0.83		
6a	0.75		
PMI	1.41	-1.01	-1.49
1b	1.01	-1.13	
4b	1.07	-1.13	
5b	1.21	-1.04	-1.60

^aRate: 0.1 V/s in CH_2Cl_2 .

spectra in frozen chloroform show no additional emission bands, and the shoulders are resolved as peaks.

The emission quantum yields, Φ , for **1a–6a** and **1b**, **4b**, and **5b** measured in dichloromethane at room temperature are in the range 0.30–0.80 (Table 2), and show that the perylenyl complexes of platinum are highly fluorescent, probably because of the weakness of the interaction of the platinum filled π -orbitals with the frontier empty π^* -orbitals of the Per or PMI fragment (see below). Similar results have been reported recently for two palladium complexes of perylene diimides, in that case attached to the bay region, which also show strong fluorescence ($\Phi = 0.65$ and 0.22).²²

The electrochemical properties of the Per and PMI derivatives have been measured in CH_2Cl_2 by cyclic voltammetry, in the range 1.6 to -1.8 V . Their voltammetric data are listed in Table 4. For Per complexes only one reversible wave was found within the range studied, at $\sim +0.75 \text{ V}$, with a decrease in the potential of at least 0.20 V, relative to perylene ($+1.06 \text{ V}$).⁴⁰ As expected, the PMI derivatives are easier to reduce because of the strong electron-accepting nature of the carboximide substituents,⁴¹ and oxidation and reduction reversible waves were observed. The neutral complexes **1b** and **4b** show one oxidation in the range $+1.01$ to $+1.07 \text{ V}$ and one reduction at $\sim -1.18 \text{ V}$. For the cationic complex **5b** the oxidation potential is $+1.21 \text{ V}$, and the first reduction potential is -1.10 V , but a second quasi-reversible reduction wave at -1.66 V is observed. Thus, compared to the parent PMI ligand, oxidation and reduction potentials appear at lower potentials, and this effect is less marked for the cationic complex **5b** than in the neutral derivatives **1b** and **4b**, suggesting that the $\text{Pt}(\text{PET}_3)_2\text{X}$ fragment (which is not directly involved in the redox process) is making the Per or PMI fragment more electron rich.¹⁷ⁱ Although the two electronic processes are different, some parallelism can be expected, at a qualitative level, between the trends observed in a series of complexes for redox processes and for luminescence energies, as seen here.

The effects of the substituents on the spectral shifts deserves a final comment, as they can be correlated to some basic features of the Pt–C bond, and to some classical parameters. The Pt–C σ bond aryl is polarized toward the carbon atom. On the other hand, the possible π back-bonding component of this bond, involving the π orbitals of Pt and the π^* orbitals of the aryl, is expected

(38) Yang, L.; Shi, M.; Wang, M.; Chen, H. *Tetrahedron* **2008**, *64*, 5404.

(39) Reisfeld, R.; Gvishi, R. *Chem. Phys. Lett.* **1993**, *213*, 338.

(40) Parker, V. D. *J. Am. Chem. Soc.* **1976**, *98*, 98.

(41) Lee, S. K.; Zu, Y.; Herrmann, A.; Geerts, Y.; Müllen, K.; Bard, A. J. *J. Am. Chem. Soc.* **1999**, *121*, 3513.

to be small for Pt (this effect has been observed in a related Pd system²²) because of the high stabilization of the d orbitals at the end of the transition metal series.⁴² Thus, the interaction of the fragments Pt(PEt₃)₂X with Per or PMI through the C–Pt bond is transmitted mainly via a σ interaction involving the 5d_z orbital of Pt, with very little π component. This does not mean that the phenomena related from electron transitions involving π ligand orbitals will not be indirectly affected, as the energy of all the orbitals of the ligand will be slightly modified by the polarization of the C–Pt bond, which in turn depends of the ancillary ligands and the charge on platinum. This destabilizing effect has been argued to be similar for the highest occupied molecular orbital (HOMO) and the lowest unoccupied molecular orbital (LUMO) of a polycyclic aromatic system, implying that no shift should be expected. However, a second consequence of the polar interaction C–Pt is that, as calculated for pyrene,^{21b} an electron rich Pt 5d_z orbital, being close but lower in energy to the HOMO of the polycyclic aromatic system will interact with it producing a reduction of the HOMO–LUMO gap. In other words, it can be expected that 5d_z orbitals of Pt with enriched nucleophilicity (higher energy) should produce higher red shifts for the polycyclic system based transitions.

Should this conception be right, the observed trends in this paper are expected to be related to other molecular properties that depend on the donor ability of the ancillary ligands and the charge on the Pt fragment. The adequate classical concepts reporting on the energy of the corresponding orbital involved in the Pt–C bond are the charge of the complex, and the trans-effect of the ancillary ligands,⁴³ which has been determined on *trans*-[PtMeX(PEt₃)₂] and follows the trend NO₃ < NCS < Br < CN, exactly in keeping with our spectroscopic trends and with the C–Pt distances in complexes **2a**, **4b**, and **5a**, supporting our interpretation.⁴⁴ Along the same line, the series of nucleophilicity of ligands toward platinum (n_{Pt}) shows the order Br < CN for neutral complexes, and py < CNC₆H₁₁ for cationic complexes.⁴⁵ Thus, the spectroscopic effects observed are perfectly compatible with the spectroscopic effects discussed above and support that the observations can be understood without π back-donation from Pt.

Conclusions

The first perylene and PMI derivatives of platinum were synthesized by attaching a Pt(PEt₃)₂X fragment (X = neutral or anionic ligand) to the perylene or PMI molecule. The compounds are soluble in common organic solvents. The metal center is σ -bonded directly to the 3 position of the perylene core. The coordination of Pt to perylene or PMI has a moderate quenching effect on the fluorescence, but the organo-platinum complexes are still highly fluorescent: the emission

quantum yield is somewhat lower for the complexes than for the precursor, but still in the same order of magnitude (many of them in the range 70–80% of the mother molecule). All the platinum complexes show a shift of the emission to lower energy as compared to the free ligands. The formation of platinum complexes with different X ligands in *trans* with respect to the perylenyl ligand has a perfectly measurable and distinct effect on the photophysical properties, although the quantitative shift is moderate because the luminescence is apparently localized on the perylene core and the platinum d orbitals have a weak interaction with the π -system of the perylenyl fragment. It seems that the spectroscopic effects of the Pt fragment are originated mostly by variations in the energy of the metal orbital involved in the C–Pt bond, induced by the ancillary ligands and the charge of the platinum complex.

Experimental Section

Materials and General Methods. All reactions were carried out under dry nitrogen. The solvents were purified according to standard procedures. Literature methods were used to prepare 3-bromoperylene,²⁴ *N*-(2,5-di-*tert*-butylphenyl)-9-bromoperylene-3,4-dicarboximide,²⁵ and [Pt(PEt₃)₄].⁴⁶ C, H, N analyses were carried out on a Perkin-Elmer 2400 microanalyzer. IR spectra (cm⁻¹) were recorded on a Perkin-Elmer FT-1720X spectrometer. ¹H and ³¹P NMR spectra were recorded on Bruker AC 300 or Bruker 400 MHz spectrophotometers in CDCl₃, with chemical shifts referred to TMS and 85% H₃PO₄, respectively. UV/vis absorption spectra were obtained on a Shimadzu UV-1603 spectrophotometer, in chloroform solution (1 × 10⁻⁵ M). Luminescence data were recorded on a Perkin-Elmer LS-luminescence spectrometer, in CHCl₃ (1 × 10⁻⁵ M) and in solid state measurements were made using finely pulverized KBr dispersions of the sample in 5 mm quartz tubes at room temperature. Luminescence quantum yields were obtained at room temperature using the optically dilute method ($A < 0.1$) in degassed dichloromethane (quantum yields standards were perylene in ethanol ($\Phi_f = 0.92$),⁴⁷ and Rhodamine B in ethanol ($\Phi_f = 0.70$), using an excitation wavelength of 409 and 510 nm, respectively, in dichloromethane).³⁶ The emission lifetime measurements were carried out with a Lifespec-red picosecond fluorescence lifetime spectrometer from Edinburgh Instruments. As excitation sources two diode lasers, with 405 and 470 nm nominal wavelengths, were used. The first wavelength (405 nm) has a pulse width of 88.5 ps, with a typical average power of 0.40 mW. The second wavelength (470 nm) has a pulse width of 97.2 ps, and its typical average power is 0.15 mW. The pulse period is 1 μ s, and the pulse repetition frequency is 10 MHz. The monochromator slit is 2 nm. The instrument response measure at the HWHM (half width at half maximum) was below 350 ps. The technique used is “Time Correlated Single Photon Counting” (TCSPC).

Electrochemical Measurements. Electrochemical studies employed cyclic voltametry using a potentiostat EG&G model 273. The three-electrode system was equipped with a platinum (3 mm diameter) working electrode, a saturated calomel reference electrode (SCE), and a Pt wire counter electrode. The electrochemical potentials were calibrated relative to SCE, using ferrocene as an internal standard (Fc/Fc⁺) at +0.46 V vs SCE). Tetra-*n*-butylammonium hexafluorophosphate (0.1 M) in CH₂Cl₂ was used as supporting electrolyte, and the solutions of the complexes were in the order 10⁻³ M.

Synthesis of 1a. To a solution of [Pt(PEt₃)₄] (0.600 g, 0.90 mmol) in 70 mL of toluene under N₂ atmosphere was added 3-bromoperylene (0.300 g, 0.90 mmol). The green solution was stirred

(42) Anderson, G. K. In *Comprehensive Organometallic Chemistry II*; Abel, E. W., Stone, F. G. A., Wilkinson, G., Eds.; Pergamon: Oxford, U.K., 1995; Vol. 9, p 445.

(43) This series is based on the observed $\nu(\text{Pt}-\text{C})$ frequencies in the IR: Appleton, T. G.; Clark, H. C.; Manzer, L. E. *Coord. Chem. Rev.* **1973**, *10*, 335.

(44) For **2a** and **4b** the distances are equal within experimental error.

(45) Tobe, M. L. In *Comprehensive Coordination Chemistry*; Wilkinson, G., Gillard, R. D., McCleverty, J. A., Eds.; Pergamon Press: Oxford, 1987; Vol. 1, p 313.

(46) Schunn, R. A. *Inorg. Chem.* **1976**, *15*, 208.

(47) Montalti, M.; Credi, A.; Prodi, L.; Gandolfini, M. T. *Handbook of Photochemistry*, 3rd ed.; CRC Press LLC: Boca Raton, FL, 2005.

12 h, then the solvent was removed in vacuum. The brown residue was washed with pentane (15 mL) and was recrystallized from dichloromethane/methanol. The brown precipitate **1a** was dried in vacuum. Yield: 0.600 g, 87%. Anal. Calcd for $C_{32}H_{41}BrP_2Pt$: C, 50.40; H, 5.42. Found: C, 50.04; H, 5.26. 1H NMR (400 MHz, $CDCl_3$): δ 8.58 (d, $J = 7.6$ Hz, H^4), 8.16 (d, $J = 7.3$ Hz, H^7), 8.13 (d, $J = 8.8$ Hz, H^{12}), 8.11 (d, $J = 7.8$ Hz, H^6), 7.80 (d, $J = 7.8$ Hz, H^1), 7.63 (d, $J = 8.8$ Hz, H^9), 7.61 (d, $J = 8.1$ Hz, H^2), 7.59 (t, $J = 8.1$ Hz, H^{11}), 7.42 (t, $J = 7.8$ Hz, H^8), 7.41 (d, H^{10}), 7.38 (t, $J = 7.6$ Hz, H^5), 1.75–1.59 (m, 12H, CH_2CH_3), 1.09–0.98 (m, 18H, CH_2CH_3). $^{31}P\{^1H\}$ NMR ($CDCl_3$): δ 12.19 (s, $J_{PPt} = 2704$ Hz). UV/vis ($CHCl_3$) λ_{max} (ϵ , $M^{-1} cm^{-1}$) = 468 (25840), 441 (33590), 418 (21510), 256 (36120). Fluorescence emission ($CHCl_3$, $\lambda_{exc} = 442$ nm) λ_{em} (I_{rel}) = 471(1) nm, 515(0.55) nm.

Synthesis of 2a. KSCN (0.010 g, 0.109 mmol) was added to the stirred solution of **1a** (0.070 g, 0.09 mmol) in 20 mL of acetone under N_2 atmosphere. After 12 h, the solvent was distilled off, and the residue was redissolved in a minimal amount of dichloromethane, and the cloudy solution was filtered through a Kieselguhr filter. Complex **2a** was precipitated by the addition of methanol (30 mL) as a yellow solid. Yield: 0.05 g, 72%. Anal. Calcd for $C_{33}H_{41}NP_2PtS$: C, 53.51; H, 5.58; N, 1.89. Found: C, 53.51; H, 5.27; N, 1.99. 1H NMR (300 MHz, $CDCl_3$): δ 8.43 (d, $J = 8.1$ Hz, 1H), 8.17–8.10 (m, 3H), 7.81 (d, $J = 7.5$ Hz, 1H), 7.65–7.59 (m, 2H), 7.50–7.38 (m, 4H), 1.64–1.46 (m, 12H, CH_2CH_3), 1.13–1.03 (m, 18H, CH_2CH_3). $^{31}P\{^1H\}$ NMR ($CDCl_3$): δ 14.56 (s, $J_{PPt} = 2740$ Hz). IR (KBr) ν ($N=C=S$) = 2099 cm^{-1} . UV/vis ($CHCl_3$) λ_{max} (ϵ , $M^{-1} cm^{-1}$) = 464 (28400), 438 (26330), 260 (33330), 240 (28622). Fluorescence emission ($CHCl_3$, $\lambda_{exc} = 464$ nm) λ_{em} (I_{rel}) = 482(1) nm, 511(0.67) nm.

Synthesis of 3a. Freshly prepared silver cyanide [obtained from $AgNO_3$ (0.020 g, 0.11 mmol) and KCN (0.080 g, 0.11 mmol)] and **1a** (0.070 g, 0.091 mmol) in acetone (20 mL) were stirred for 12 h in the dark, under N_2 atmosphere. The solvent was then evaporated, the residue was redissolved in dichloromethane (ca. 20 mL), and the cloudy solution was filtered through a Kieselguhr filter. The yellow solid **3a** was precipitated by the addition of 30 mL of methanol. Yield: 0.05 g, 78%. Anal. Calcd for $C_{33}H_{41}NP_2Pt$: C, 55.93; H, 5.83; N, 1.89. Found: C, 55.57; H, 5.55; N, 1.75. 1H NMR (300 MHz, $CDCl_3$): δ 8.24 (d, $J = 8.0$ Hz, 1H), 8.16–8.09 (m, 3H), 7.90 (d, $J = 7.5$ Hz, 1H), 7.64–7.58 (m, 2H), 7.49–7.35 (m, 4H), 1.76–1.62 (m, 12H, CH_2CH_3), 1.12–1.01 (m, 18H, CH_2CH_3). $^{31}P\{^1H\}$ NMR ($CHCl_3$): δ 11.16 (s, $J_{PPt} = 2590$ Hz). IR (KBr) ν ($N=C$) = 2116 cm^{-1} . UV/vis ($CHCl_3$) λ_{max} (ϵ , $M^{-1} cm^{-1}$) = 463 (31730), 437 (29100), 257 (38700), 240 (24910). Fluorescence emission ($CHCl_3$, $\lambda_{exc} = 462$ nm) λ_{em} (I_{rel}) = 479(1) nm, 510(0.65) nm.

Synthesis of 4a. Complex **1a** (0.250 g, 0.33 mmol) and $AgNO_3$ (0.060 g, 0.33 mmol) in 60 mL of acetone under N_2 atmosphere were placed in a Schlenk flask. The reaction was stirred for 3 h in the dark, after which the reaction mixture was evaporated to dryness. The residue was redissolved in dichloromethane (ca. 20 mL), and the cloudy solution was filtered through a Kieselguhr filter. The brown solid **4a** was precipitated by the addition of methanol. Yield: 0.200 g, 81%. Anal. Calcd for $C_{32}H_{41}NO_3P_2Pt$: C, 51.61; H, 5.55; N, 1.88. Found: C, 51.21; H, 5.20; N, 1.76. 1H NMR (300 MHz, $CDCl_3$): δ 8.74 (d, $J = 7.9$ Hz, 1H), 8.18–8.12 (m, 3H), 7.79 (d, $J = 7.9$ Hz, 1H), 7.66–7.39 (m, 6H), 1.55–1.40 (m, 12H, CH_2CH_3), 1.13–1.03 (m, 18H, CH_2CH_3). $^{31}P\{^1H\}$ NMR ($CDCl_3$): δ 17.24 (s, $J_{PPt} = 2841$ Hz). UV/vis ($CHCl_3$) λ_{max} (ϵ , $M^{-1} cm^{-1}$) = 464 (28750), 438 (25960), 260 (27010), 253 (26490). Fluorescence emission ($CHCl_3$, $\lambda_{exc} = 467$ nm) λ_{em} (I_{rel}) = 488(1) nm, 517(0.67) nm.

Synthesis of 5a. To a suspension of **4a** (0.080 g, 0.107 mmol) in 20 mL of acetone/water (1:1) under N_2 atmosphere was added CN^tBu (24 μL , 0.21 mmol). The solution was stirred for 12 h, and then KPF_6 (0.040 g, 0.21 mmol) was added. The reaction mixture was concentrated and a yellow solid precipitated, which

was filtered and washed with H_2O (2×3 mL). The solid was redissolved in dichloromethane (20 mL), and the solution dried with magnesium sulfate. The solution was filtered, and the solvent was then removed in vacuum, yielding **5a** as a yellow solid. Yield: 0.085 g, 86%. Anal. Calcd for $C_{37}H_{50}NF_6P_3Pt$: C, 48.79; H, 5.53; N, 1.54. Found: C, 48.74; H, 5.37; N, 1.46. 1H NMR (400 MHz, acetone- d_6): δ 8.34 (d, $J = 7.4$ Hz, H^9), 8.30 (d, $J = 8.3$ Hz, H^8), 8.27 (d, $J = 9.0$ Hz, H^3), 8.16 (d, $J = 8.2$ Hz, H^{11}), 8.13 (d, $J = 7.7$ Hz, H^2), 7.75 (d, $J = 8.1$ Hz, H^6), 7.72 (d, $J = 8.3$ Hz, H^5), 7.54 (d, $J = 7.6$ Hz, H^1), 7.51 (t, $J = 7.9$ Hz, H^7), 7.50 (t, $J = 8.0$ Hz, H^{10}), 7.48 (t, $J = 7.9$ Hz, H^4), 1.8–1.6 (m, 21H, CH_2CH_3 , CN^tBu), 1.13–1.05 (m, 18H, CH_2CH_3). $^{31}P\{^1H\}$ NMR ($CHCl_3$): δ 12.32 (s, $J_{PPt} = 2413$ Hz), –143.73 (septuplet, $J_{PF} = 713$ Hz). IR (KBr, cm^{-1}): ν 2196 ($C\equiv N$). UV/vis ($CHCl_3$) λ_{max} (ϵ , $M^{-1} cm^{-1}$) = 456 (38040), 429 (30920), 259 (50960). Fluorescence emission ($CHCl_3$, $\lambda_{exc} = 456$ nm) λ_{em} (I_{rel}) = 467(1) nm, 496(0.59) nm.

Synthesis of 6a. To a suspension of **4a** (0.040 g, 0.053 mmol) in 5 mL of acetone and in 5 mL of H_2O under N_2 atmosphere was added 4-methylpyridine (5 μL , 0.21 mmol). The solution was stirred for 12 h, then KPF_6 (0.020 g, 0.11 mmol) was added. The reaction mixture was concentrated, and a yellow solid precipitated. The precipitate was filtered and washed with H_2O (2×3 mL). The solid was redissolved in dichloromethane (20 mL), and the solution dried with magnesium sulfate. The solution was filtered, and the solvent was then removed in vacuum, yielding **6a** as a yellow solid. Yield: 0.03 g, 62%.

Anal. Calcd for $C_{38}H_{48}NF_6P_3Pt$: C, 49.57; H, 5.25; N, 1.52. Found: C, 49.37; H, 5.16; N, 1.41. 1H NMR (400 MHz, $CDCl_3$): δ 8.71 (d, $J = 5.8$ Hz, 1H), 8.60 (d, $J = 5.5$, 1H), 8.55 (d, $J = 8.06$, 1H), 8.19–8.15 (m, 3H), 7.90 (d, $J = 7.5$ Hz, 1H), 7.68–7.43 (m, 8H), 2.54 (s, 3H, CH_3), 1.27–1.21 (m, 12H, CH_2CH_3), 1.09–1.01 (m, 18H, CH_2CH_3). $^{31}P\{^1H\}$ NMR ($CHCl_3$): δ 11.74 (s, $J_{PPt} = 2662$ Hz), δ –143.71 (septuplet, $J_{PF} = 712$ Hz). UV/vis ($CHCl_3$) λ_{max} (ϵ , $M^{-1} cm^{-1}$) = 460 (33370), 432 (27540), 260 (46400). Fluorescence emission ($CHCl_3$, $\lambda_{exc} = 459$ nm) λ_{em} (I_{rel}) = 473(1) nm, 501(0.62) nm.

Synthesis of 1b. To a solution of $[Pt(PEt_3)_4]$ (0.113 g, 0.17 mmol) in THF (20 mL) under a N_2 atmosphere was added *N*-(2,5-di-*tert*-butylphenyl)-9-bromo-perylene-3,4-dicarboximide (0.100 g, 0.17 mmol). The red solution was stirred 6 h, then the solvent was removed in vacuum. The purple residue was washed with pentane (3×15 mL) and recrystallized from $CH_2Cl_2/MeOH$. The purple precipitate **2b** was dried in vacuum. Yield: 0.130 g, 75%. Anal. Calcd for $C_{48}H_{60}NBRO_2P_2Pt$: C, 56.53; H, 5.13; N, 1.37. Found: C, 56.27; H, 5.40; N, 1.37. 1H NMR (400 MHz, $CDCl_3$): δ 8.87 (d, $J = 8.3$ Hz, H^4), 8.63 (d, $J = 8.1$ Hz, H^7), 8.60 (d, $J = 8.1$ Hz, H^{11}), 8.47 (d, $J = 8.3$ Hz, H^6), 8.46 (d, $J = 8.1$ Hz, H^8), 8.41 (d, $J = 8.3$ Hz, H^{12}), 8.08 (d, $J = 7.9$ Hz, H^1), 7.86 (d, $J = 7.5$ Hz, H^2), 7.60 (t, $J = 8.1$ Hz, H^5), 7.58 (d, $J = 8.5$ Hz, H^{13}), 7.45 (dd, $J = 8.4$, $J = 2.2$ Hz, H^{14}), 7.05 (d, $J = 2.2$, H^{15}), 1.73–1.60 (m, 12H, CH_2CH_3), 1.33 (s, 9H, tBu), 1.28 (s, 9H, tBu), 1.10–1.02 (m, 18H, CH_2CH_3). $^{31}P\{^1H\}$ NMR ($CDCl_3$): δ 12.12 (s, $J_{PPt} = 2666$ Hz). IR (KBr, cm^{-1}): ν 1699 ($C=O$), 1657 ($C=O$). UV/vis ($CHCl_3$) λ_{max} (ϵ , $M^{-1} cm^{-1}$) = 543 (38840), 275 (82920), 241 (59530). Fluorescence emission ($CHCl_3$, $\lambda_{exc} = 542$ nm) λ_{em} (I_{rel}) = 618(1) nm, 659(0.65) nm.

Synthesis of 4b. A mixture of **1b** (0.250 g, 0.26 mmol) and $AgNO_3$ (0.050 g, 0.29 mmol) in 50 mL of acetone, under N_2 atmosphere and shielded from light, was stirred 2 h, then the solvent was removed in vacuum. The solid was redissolved in dichloromethane, and the cloudy solution was filtered through a Kieselguhr filter. The purple solid **4b** was precipitated by addition of diethyl ether. Yield: 0.211 g, 86%. Anal. Calcd for $C_{48}H_{60}N_2O_5P_2Pt$: C, 61.33; H, 6.43; N, 2.98. Found: 61.08; H, 6.30; N, 2.74. 1H NMR (400 MHz, $CDCl_3$): δ 9.02 (d, $J = 8.3$ Hz, H^4), 8.63 (d, $J = 8.1$ Hz, H^7), 8.60 (d, $J = 8.1$ Hz, H^{11}), 8.48 (d, $J = 8.1$ Hz, H^8), 8.46 (d, $J = 8.1$ Hz, H^6), 8.41 (d, $J = 8.1$ Hz, H^{12}), 8.06 (d, $J = 7.8$ Hz, H^1), 7.77 (d, $J = 7.8$ Hz, H^2), 7.66 (d, $J = 7.8$ Hz, H^5), 7.58 (d, $J = 8.6$ Hz, H^{13}),

Table 5. Crystal and Structure Refinement Data for **2a**, **5a**, and **4b**

	2a	4b	5a ·CH ₂ Cl ₂
empirical formula	C ₃₃ H ₄₁ NP ₂ PtS	C ₄₈ H ₆₀ N ₂ O ₅ P ₂ Pt	C ₃₈ H ₅₂ Cl ₂ F ₆ NP ₃ Pt
formula weight	740.76	1002.01	995.71
temperature (K)	298(2)	298(2)	298(2)
wavelength (Å)	0.71073	0.71073	0.71073
crystal system	monoclinic	monoclinic	monoclinic
space group	<i>P2(1)/n</i>	<i>P2(1)/n</i>	<i>P2(1)/n</i>
<i>a</i> (Å)	10.2893(16)	14.047(3)	17.077(8)
<i>b</i> (Å)	14.623(2)	19.975(4)	14.366(7)
<i>c</i> (Å)	21.444(3)	16.215(3)	17.372(8)
α (deg)	90	90	90
β (deg)	100.554(3)	90.672(3)	99.957(9)
γ (deg)	90	90	90
<i>V</i> (Å ³)	3171.9(8)	4549.7(14)	4198(3)
<i>Z</i>	4	4	4
<i>D</i> _{calc} (g cm ⁻³)	1.551	1.463	1.576
absorpt. coefficient (mm ⁻¹)	4.613	3.201	3.639
<i>F</i> (000)	1480	2040	1992
crystal size (mm)	0.21 × 0.06 × 0.05	0.37 × 0.11 × 0.10	0.41 × 0.30 × 0.07
θ range for data collection	1.69 to 26.37°	1.62 to 26.38°	1.84 to 27.50°
reflections collected	27124	39476	39268
independent reflections	6473	9311	9643
absorption correction	SADABS	SADABS	SADABS
maximum and minimum transmission factor	0.7940 and 0.5489	1.000000 and 0.663169	0.9806 and 0.5628
data/restraints/parameters	6473/231/398	9311/0/535	9643/16/489
goodness-of-fit on <i>F</i> ²	1.007	1.030	1.020
<i>R</i> ₁ [<i>I</i> > 2σ(<i>I</i>)]	0.0554	0.0347	0.0446
<i>wR</i> ₂ (all data)	0.1706	0.0963	0.1197

7.44 (dd, *J* = 8.6 Hz, *J* = 2.0 Hz, H¹⁴), 7.04 (d, *J* = 2.2 Hz, H¹⁵), δ 1.52–1.37 (m, 12H, CH₂CH₃), δ 1.33 (s, 9H, ^tBu), δ 1.28 (s, 9H, ^tBu), δ 1.15–1.06 (m, 18H, CH₂CH₃). ³¹P{¹H} NMR (CDCl₃): δ 17.02 (s, *J*_{Pt} = 2795 Hz). IR (KBr, cm⁻¹): ν = 1699 (C=O), 1656 (C=O). UV/vis (CHCl₃) λ_{max} (ε, M⁻¹ cm⁻¹) = 545 (36650), 276 (59300). Fluorescence emission (CHCl₃, λ_{exc} = 542 nm) λ_{em}(*I*_{rel}) = 619(1) nm, 660(0.50) nm.

Synthesis of 5b. To a suspension of **4b** (0.080 g, 0.08 mmol) in 10 mL of acetone and 10 mL of H₂O under N₂ atmosphere was added CN^tBu (18 μL, 0.16 mmol). The red solution was stirred for 12 h and then KPF₆ (0.040 g, 0.21 mmol) was added. After 30 min, the reaction mixture was concentrated, and a red solid precipitated, which was filtered and washed with H₂O (2 × 3 mL). The solid was redissolved in CH₂Cl₂, and the solution dried with magnesium sulfate. The solution was filtered, and the solvent was then removed in vacuum. The solid was recrystallized from CH₂Cl₂/diethyl ether affording a red precipitate **5b**, which was vacuum-dried. Yield: 0.069 g, 79%. Anal. Calcd for C₅₃H₆₉N₂F₆O₂P₃Pt: C, 54.50; H, 5.95; N, 2.40. Found: C, 54.20; H, 5.77; N, 2.23. ¹H NMR (400 MHz, CD₂Cl₂): δ 8.61 (d, *J* = 8.3 Hz, H⁷), 8.59 (d, *J* = 8.1 Hz, H¹¹), 8.52 (d, *J* = 8.3 Hz, H⁸), 8.51 (d, *J* = 8.3 Hz, H⁹), 8.49 (d, *J* = 8.3 Hz, H¹²), 8.29 (d, *J* = 7.6 Hz, H¹), 8.25 (d, *J* = 8.1 Hz, H⁴), 7.67 (t, *J* = 7.8 Hz, H³), 7.60 (d, *J* = 8.6 Hz, H²), 7.60 (d, *J* = 8.6 Hz, H¹⁵), 7.48 (dd, *J* = 2.3 Hz, *J* = 8.6 Hz, H¹⁴), 7.03 (d, *J* = 2.3 Hz, H¹³), 1.8–1.6 (m, 21H, CH₂CH₃, CN^tBu), 1.33 (s, 9H, ^tBu), 1.28 (s, 9H, ^tBu), 1.15–1.06 (m, 18H, CH₂CH₃). ³¹P{¹H} NMR (CHCl₃): δ 11.75 (s, *J*_{Pt} = 2382 Hz), –143.69 (septuplet, *J*_{PF} = 713 Hz). IR (KBr, cm⁻¹): ν 2194 (C≡N), 1699 (C=O), 1656 (C=O). UV/vis (CHCl₃) λ_{max} (ε, M⁻¹ cm⁻¹) = 515 (42350), 271 (34220), 243 (43350). Fluorescence emission (CHCl₃, λ_{exc} = 517 nm) λ_{em}(*I*_{rel}) = 581(1) nm, 620(0.55) nm.

X-ray Crystal Structure Analysis. Single crystals of **2a** suitable for X-ray diffraction studies were obtained from slow diffusion of hexane into a dichloromethane solution of the crude products at –20 °C, under nitrogen. Crystals from **4b** and **5a**·CH₂Cl₂ were grown from slow diffusion of Et₂O into a dichloromethane solution of the products at –20 °C, under N₂ atmosphere. Data were taken on a Bruker AXS SMART 1000 CCD diffractometer, using φ and ω scans, MoK_α radiation (λ = 0.71073 Å), graphite monochromator, and *T* = 298 K. Raw frame data were integrated with SAINT⁴⁸ program. Structures (Table 5) were

solved by direct methods with SHELXTL.⁴⁹ Semiempirical absorption correction was made with SADABS.⁵⁰ All non-hydrogen atoms were refined anisotropically. Hydrogen atoms were set in calculated positions and refined as riding atoms, with a common thermal parameter. All calculations were made with SHELXTL. In the structures of compounds **2a** and **4b** it was found that the ethyl groups of the PET₃ ligands were affected by disorder, which was possible to model in some cases. More details are given in the Supporting Information and cif file. Crystallographic data (excluding structure factors) for the structures reported in this paper have been deposited with the Cambridge Crystallographic Data Centre as Supplementary publications with the following deposition numbers: CCDC 759812, 759813, and 759814 for complexes **2a**, **4b**, and **5a**, respectively. These data can be obtained free of charge from The Cambridge Crystallographic Data Centre via www.ccdc.cam.ac.uk/data_request/cif.

Acknowledgment. We thank Dr. Emilio Palomares and Dr. Javier Pérez for some spectral measurements, Prof. Dr. Larry Falvello for advice in the resolution of the X-ray diffraction structures, and the Spanish Comisión Interministerial de Ciencia y Tecnología (CTQ2008-03954/BQU and MAT2008-06522-C02-02), INTECAT Consolider Ingenio 2010 (CSD2006-0003), and the Junta de Castilla y León (Project VA012A08 and GR169) for financial support.

Supporting Information Available: Intermolecular contacts detected in **4b**, split Figure 2-above in two, absorption and emission spectra of **1a** and **1b** in different solvents, excitation spectra, Cyclic voltammogram of compounds **1a** and **5b**, and refinement details of the X-ray Crystal Structure Analysis of **2a** and **5a**. This material is available free of charge via the Internet at <http://pubs.acs.org>.

(48) SAINT+; SAX area detector integration program, Version 6.02; Bruker AXS, Inc.: Madison, WI, 1999.

(49) Sheldrick, G. M. SHELXTL, An integrated system for solving, refining, and displaying crystal structures from diffraction data, Version 5.1; Bruker AXS, Inc.: Madison, WI, 1998.

(50) Sheldrick, G. M. SADABS, Empirical Absorption Correction Program; University of Göttingen: Göttingen, Germany, 1997.